Cell Stem Cell
Article

Tet and TDG Mediate DNA Demethylation Essential for Mesenchymal-to-Epithelial Transition in Somatic Cell Reprogramming

Xiao Hu,[1,5] Lei Zhang,[1,5] Shi-Qing Mao,[1,5] Zheng Li,[1] Jiekai Chen,[2] Run-Rui Zhang,[1] Hai-Ping Wu,[1] Juan Gao,[1] Fan Guo,[1] Wei Liu,[1] Gui-Fang Xu,[1] Hai-Qiang Dai,[1] Yujiang Geno Shi,[3] Xianlong Li,[4] Boqiang Hu,[4] Fuchou Tang,[4] Duanqing Pei,[2] and Guo-Liang Xu[1,*]

[1]Shanghai Key Laboratory of Molecular Andrology, The State Key Laboratory of Molecular Biology, Institute of Biochemistry and Cell Biology, Shanghai Institutes for Biological Sciences, Chinese Academy of Sciences, Shanghai 200031, China
[2]CAS Key Laboratory of Regenerative Biology, South China Institute for Stem Cell Biology and Regenerative Medicine, Guangzhou Institutes of Biomedicine and Health, Chinese Academy of Sciences, Guangzhou 510530, China
[3]Division of Endocrinology, Diabetes, and Hypertension, Department of Medicine and BCMP, Brigham and Women's Hospital and Harvard Medical School, Boston, MA 02115, USA
[4]Biodynamic Optical Imaging Center, College of Life Sciences, Peking University, Beijing 100871, China
[5]These authors contributed equally to this work
*Correspondence: glxu@sibs.ac.cn
http://dx.doi.org/10.1016/j.stem.2014.01.001

SUMMARY

Tet-mediated DNA oxidation is a recently identified mammalian epigenetic modification, and its functional role in cell-fate transitions remains poorly understood. Here, we derive mouse embryonic fibroblasts (MEFs) deleted in all three *Tet* genes and examine their capacity for reprogramming into induced pluripotent stem cells (iPSCs). We show that Tet-deficient MEFs cannot be reprogrammed because of a block in the mesenchymal-to-epithelial transition (MET) step. Reprogramming of MEFs deficient in TDG is similarly impaired. The block in reprogramming is caused at least in part by defective activation of key miRNAs, which depends on oxidative demethylation promoted by Tet and TDG. Reintroduction of either the affected miRNAs or catalytically active Tet and TDG restores reprogramming in the knockout MEFs. Thus, oxidative demethylation to promote gene activation appears to be functionally required for reprogramming of fibroblasts to pluripotency. These findings provide mechanistic insight into the role of epigenetic barriers in cell-lineage conversion.

INTRODUCTION

Pluripotent cells, such as those in early embryos, proliferate and differentiate into distinctive cell lineages. Lineage commitment is established and maintained in development by epigenetic programming of gene-expression profiles, in which DNA methylation plays a prominent role (Goll and Bestor, 2005; Jaenisch and Bird, 2003). DNA methylation patterns are faithfully propagated in cells undergoing mitosis. Early embryonic genes, such as the pluripotency genes *Oct4* and *Nanog*, undergo silencing and de novo DNA methylation in their promoter and enhancer regions during cell differentiation and maintain their hypermethylated states in differentiated somatic cells (Epsztejn-Litman et al., 2008; Li et al., 2007). The developmental and cell-differentiation processes therefore entail dynamic regulation of genomic methylation accompanied by gene-expression changes.

Lineage commitment can be reversed in vivo and in vitro through natural and experimental reprogramming such as nuclear transfer of a somatic nucleus into an enucleated oocyte and factor-induced conversion of somatic cells to induced pluripotent stem cells (iPSCs). Because each cell identity is supposedly defined by a unique methylation profile that underpins its lineage commitment and serves as a barrier between different cell types, methylation reprogramming is a mechanistically vital process underlying cell-type switch. For example, demethylation of pluripotency genes is a hallmark of somatic-cell reprogramming into a pluripotent state (Gurdon and Melton, 2008; Takahashi and Yamanaka, 2006). Transcriptional activation of epigenetically silenced genes thus necessitates the demethylation of critical regulatory elements in DNA during experimental reprogramming.

The Tet family of DNA dioxygenases catalyzes oxidation of methylcytosines to hydroxymethylcytosines (5hmC), formylcytosines (5fC), and carboxylcytosines (5caC) (He et al., 2011; Ito et al., 2011; Tahiliani et al., 2009). An active mode of DNA demethylation has been proposed to encompass Tet-mediated oxidation of methylcytosines and excision of the higher oxidation products by DNA glycosylase TDG (He et al., 2011; Pastor et al., 2013; Seisenberger et al., 2013). However, the possibility of replication-associated passive dilution of 5-methylcytosine (5mC) and its oxidation products (Inoue and Zhang, 2011) has complicated the dissection of the role of Tet-initiated active demethylation in development and cell reprogramming. Whereas overexpression of Tet1 and Tet2 has been shown to promote iPSC formation through the reactivation of silenced pluripotency genes (Bagci and Fisher, 2013; Costa et al., 2013; Doege et al., 2012), the importance of and mechanism behind the Tet-mediated oxidation in cell reprogramming have remained largely undefined.

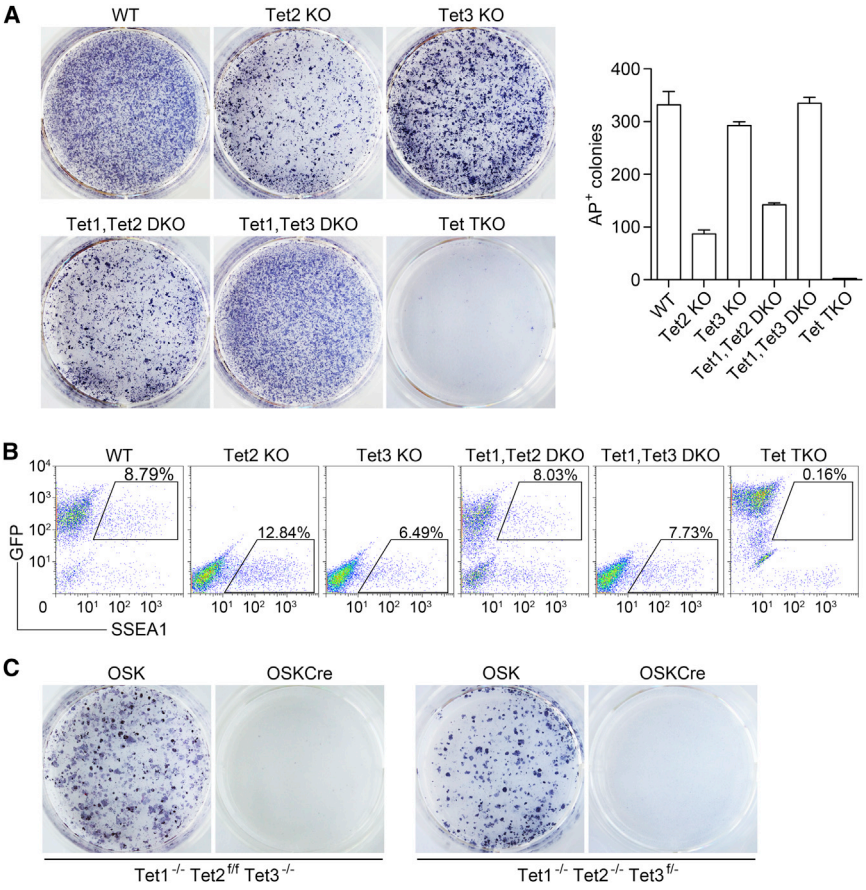

Figure 1. Tet Triple Knockout Prevents Reprogramming of MEFs

(A) Alkaline phosphatase (AP) staining of cells 10 days after retroviral transduction of Oct4, Sox2, and Klf4 (OSK). Wild-type (WT), Tet2 KO, Tet3 KO, Tet1,Tet2 double knockout (DKO), Tet1,Tet3 DKO, and Tet1,Tet2,Tet3 triple knockout (TKO) MEFs were assayed for iPSC formation. AP-positive colony numbers are shown on the right. Data represent means ± SD of three independent experiments.

(B) FACS analysis of SSEA1-positive cells at reprogramming day 10. WT, Tet1,Tet2 DKO, and TKO MEFs were sorted from chimera embryos injected with GFP-labeled ESCs. Other MEF types were isolated from homozygous embryos generated by mating heterozygotes. SSEA1-positive cells induced from each MEF type are those within polygon gates.

(C) No AP-positive colonies were generated from [Tet2-floxed, Tet1,Tet3 DKO] and [Tet3-floxed, Tet1,Tet2 DKO] MEFs upon acute deletion of Tet2 or Tet3 by Cre expression.

See also Figures S1 and S2.

In this study, we generated mouse embryonic fibroblasts (MEFs) deleted of components of the putative active DNA demethylation pathway and tested these MEFs for iPSC induction and the reactivation of genes critical for cellular reprogramming. We demonstrate here that demethylation promoted by Tet and TDG is directly involved and essential in the reactivation of miRNAs that enables a mesenchymal-to-epithelial transition to initiate the reprogramming process.

RESULTS

Tet Dioxygenases Are Essential for Fibroblasts to Undergo Reprogramming

Although Tet1 and Tet2 have been shown to facilitate cell reprogramming (Costa et al., 2013; Doege et al., 2012), it remains unclear whether Tet-mediated DNA oxidation is essential for this process. To assess the functional importance of Tet enzymes, we generated mouse embryonic fibroblasts from embryonic stems cells (ESCs) deficient in Tet genes for the generation of iPSCs (see Supplemental Experimental Procedures available online). ESCs lacking all three *Tet* genes seemed normal in self-renewal and pluripotency (Figure S1). MEFs generated from chimeric embryos with blastocyst injection of these ESCs proliferated at a similar rate as wild-type control MEFs and those isolated from homozygous embryos resulting from heterozygous mating (Figure S2A). Considering the dynamic expression of three Tet genes during iPSC generation (Figure S2B), we determined and compared the reprogramming efficiency among MEFs deficient in a single *Tet* gene and in combinations, using the three-factor (Oct4, Sox2, and Klf4) induction system (Figure S2C). MEFs with Tet1 deletion had slightly increased reprogramming efficiency as described (Chen et al., 2013), and inactivation of Tet3 had little effect, based on the comparison of alkaline phosphatase (AP)-positive colony numbers (Figure 1A). Although inactivation of Tet2 reduced the reprogramming by ~70%, AP-positive colonies could still appear. In addition, MEFs from Tet1,Tet2 and Tet1,Tet3 double knockouts also generated numerous colonies and SSEA1-positive cells. Strikingly, inactivation of all three *Tet* genes completely abolished the reprogramming potential of MEFs as evidenced by the failure to obtain AP- (Figure 1A) and SSEA1-positve cells (Figure 1B). The resistance of triple knockout (TKO) MEFs to reprogramming was further validated using high-performance engineered factors (Wang et al., 2011) in the presence of c-Myc and improved medium (Chen et al., 2011; Figure S2D). The reprogramming deficiency of TKO MEFs could not be ascribed to inherent genomic or epigenomic alterations potentially arisen from the constitutive Tet deletion, because AP-positive colonies also did not appear upon the acute deletion of Tet2 from the Tet1,Tet3 double knockout (DKO) MEFs or the acute deletion of Tet3 from Tet1,Tet2 DKO MEFs by the Cre recombinase expression (Figure 1C). Moreover, Tet TKO MEFs could be rescued for reprogramming in latter experiments. These observations indicate that the Tet enzymes are indispensable for factor-driven reprogramming of somatic cells.

Tet TKO MEFs Fail to Undergo Mesenchymal-to-Epithelial Transition during Reprogramming

Factor-driven reprogramming is a multistep process initiated by mesenchymal-to-epithelial transition (MET) as an essential event

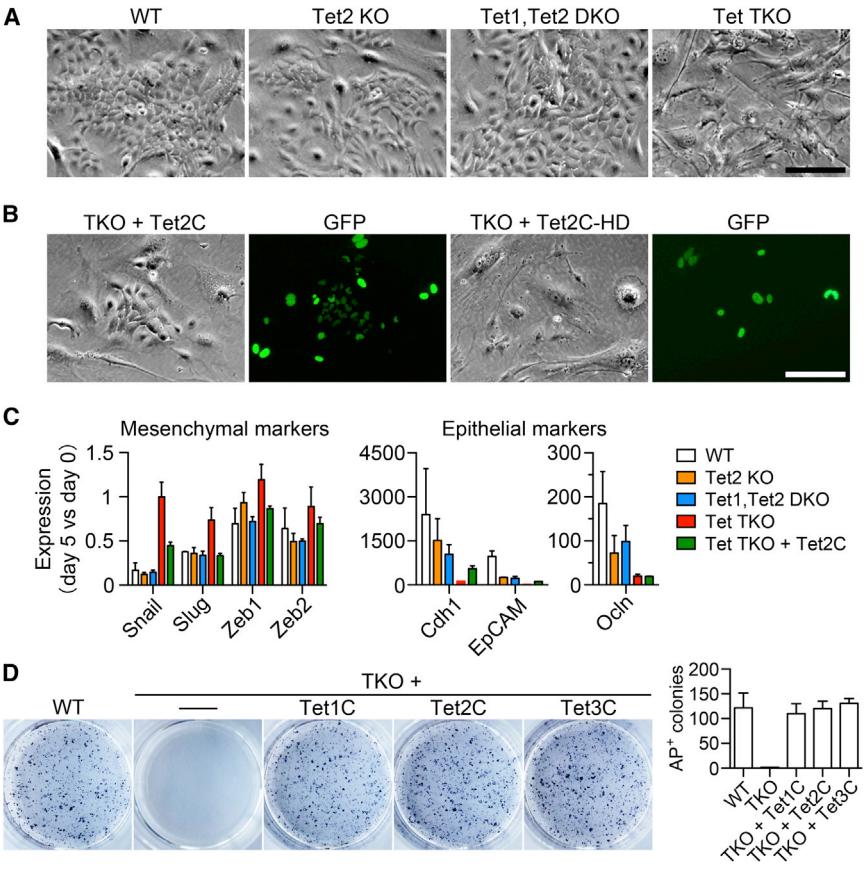

Figure 2. Tet-Deficient MEFs Are Unable to Initiate Mesenchymal-to-Epithelial Transition during Reprogramming

(A) Phase-contrast photographs of cells under reprogramming (day 5) showing lack of the morphologic shift characteristic of MET in Tet TKO MEFs. The scale bar represents 100 μm.

(B) Rescue of MET in TKO MEFs by ectopic expression of the Tet2 C-terminal catalytic domain (Tet2C). The MEFs used were derived from TKO ESCs labeled with lentiviral H2B-enhanced GFP (EGFP). Tet2C-HD carries two point mutations in the active site of the enzyme. The scale bar represents 100 μm.

(C) Failed downregulation of mesenchymal and upregulation of epithelial markers in Tet TKO MEFs as demonstrated by qRT-PCR. The expression levels were normalized to *Gapdh*. Data represent means ± SD of three independent experiments.

(D) AP staining of colonies from WT MEFs, Tet TKO MEFs, and TKO MEFs transduced with the indicated Tet at reprogramming day 10. AP-positive colony numbers are shown on the right. Data represent means ± SD of three independent experiments.

for MEFs to be successfully reprogrammed into iPSCs (Li et al., 2010; Samavarchi-Tehrani et al., 2010). The fact that AP and SSEA1, markers of early reprogramming, were not induced in TKO MEFs suggested an early reprogramming defect. Indeed, Tet TKO MEFs showed no sign of epithelium-like morphological shift, whereas wild-type, single, or double knockout MEFs exhibited an obvious MET, starting from day 4 after transduction of the Oct4, Sox2, and Klf4 (OSK) reprogramming factors (Figures 2A and S2C). The MET process in TKO MEFs could be rescued by ectopic expression of the wild-type catalytic domain, but not the inactive form of Tet2 (Figure 2B).

E-cadherin (Cdh1), EpCAM, and occludin (Ocln) are components of epithelial cell junctions, and without their expression, cells are unable to form colonies. Snail, Slug, Zeb1, and Zeb2 are transcription factors that promote the epithelial-mesenchymal transition (EMT) and maintain the mesenchymal phenotype by directly repressing epithelial gene expression (Thiery et al., 2009). Quantitative RT-PCR (qRT-PCR) analysis confirmed persistent expression of the mesenchymal markers *Snail*, *Slug*, *Zeb1*, and *Zeb2* and lack of activation of the epithelial markers *Cdh1*, *EpCAM*, and *Ocln* in Tet-deficient MEFs (Figure 2C), indicating a resistance to MET at the molecular level. The reprogramming capacity of the TKO MEFs appeared to be fully restored by ectopic expression of the catalytic domain from any of the Tet proteins (Figure 2D). Our data suggest that Tet-deficient MEFs fail to initiate the MET process due to their inability to downregulate the key mesenchymal regulators and that MET depends on the catalytic function of Tet enzymes.

Tet-Deficient MEFs Fail to Reactivate MicroRNAs Critical for MET

The miR-200 s, miR-200a, miR-200b, miR-200c, miR-141, and miR-429 are causatively involved in both cancer metastasis and experimental cell reprogramming by modulating the expression of transcription factors such as Zeb1 and Zeb2 that repress epithelial markers including E-cadherin (Gregory et al., 2008; Samavarchi-Tehrani et al., 2010; Wang et al., 2013). We confirmed that all five members of the miR-200 family were substantially upregulated in MEFs undergoing reprogramming (Figure 3A). Interestingly, the expression of miR-200 family was diminishing in Tet-deficient MEFs, most severely in TKO cells (Figure 3B). Remarkably, ectopic expression of miR-200c in the TKO MEFs restored the MET process as evident in the cell morphology, formation of colonies, and epithelial marker expression (Figures 3C and 3D). In fact, each of the three miR-200 members tested, but not the two independent miR-200c mutants containing base changes in the miRNA seed region, enabled a marked rescue in terms of AP-positive colony and SSEA-positive cell numbers (Figures 3E and 3F). Combination of the five members led to a rescue of up to 80% of the reprogramming efficiency of the wild-type MEFs (Figure 3F). Importantly, iPSC lines could be established from the TKO MEFs upon miR-200 rescue. These iPSCs displayed the typical ESC morphology (Figures 3G and 3H) and expressed endogenous pluripotency genes at similar levels as in ESCs (Figure 3I). When injected into mouse blastocysts, they contributed to the generation of chimeric embryos (Figure 3J) and to the germline in embryonic gonads (Figure 3K).

To investigate whether the failure in MET is indeed the major reason for reprogramming deficiency of TKO MEFs, we derived two types of epithelium-like cells, keratinocytes and neural

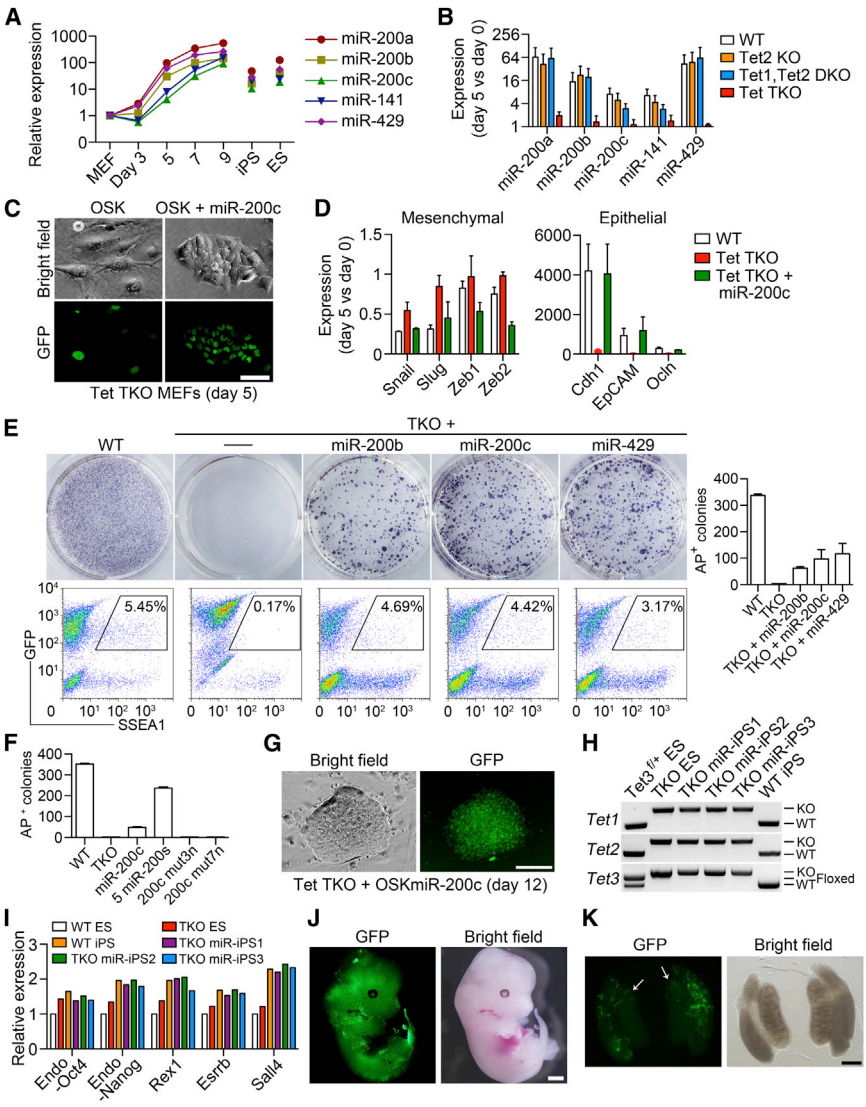

Figure 3. Impediment to Activation of miRNAs Crucial for MET in Tet-Deficient MEFs

(A) Activation of the miR-200 family miRNAs during reprogramming. Expression levels normalized to *Rnu6* are relative to the value in untransduced MEFs which is set to 1.

(B) Failed upregulation of the miR-200 family miRNAs in Tet-deficient MEFs transduced with OSK (day 5). Data represent means ± SD of two independent experiments.

(C) Restoration of MET in Tet-deficient MEFs by ectopic expression of miR-200c. Representative photographs of cells under induction with OSK alone and together with the ectopic expression of miR-200c (day 5) are shown. Nuclear H2B-GFP identifies Tet-deficient MEFs originally from the labeled TKO ESCs. The scale bar represents 50 μm.

(D) Downregulation of mesenchymal genes and upregulation of epithelial genes in TKO MEFs undergoing OSK-driven reprogramming in the presence of ectopic miR-200c. Data represent means ± SD of two independent experiments.

(E) AP (upper) and SSEA1 (lower) staining of cells from indicated MEFs rescued with miR-200b, miR-200c, or miR-429 at reprogramming day 10. Wild-type MEFs and TKO MEFs without ectopic miRNA expression were used for comparison. AP-positive colony numbers are shown on the right. Data represent means ± SD of two independent experiments.

(F) Rescue assay with five miRNAs in combination and miR-200c mutants. AP-positive colonies emerged from WT and TKO MEFs without and with the rescue by indicated miRNAs were scored at reprogramming day 10. mut3n and mut7n are two mutants of miR-200c, harboring 3- and 7-base change, respectively, in the seed region.

(G) Formation of iPSC colonies from TKO MEFs rescued for MET with ectopic miR-200c. GFP expression confirms the cell origin from TKO ESCs used to generate MEFs. The scale bar represents 80 μm.

(H) Genotype confirmation of three independent TKO iPSC lines 1–3 (denoted as miR-iPSC). Genomic PCR of Tet3f/+ iPSCs, TKO ESCs, and wild-type iPSCs provides controls for identifying the bands representing the WT and knockout (KO) alleles of the three *Tet* genes.

(I) Expression of pluripotency markers in Tet TKO miR-iPSCs.

(J) Chimera formation assay. Representative images of whole-mount embryos of E12.5 are shown. Note that green fluorescent cells were from GFP-labeled Tet TKO miR-iPSCs. The scale bar represents 1 mm.

(K) Representative images of chimeric genital ridges isolated from an E12.5 embryo. GFP-positive cells (arrows) identify those originally from Tet TKO miR-iPSCs. The scale bar represents 200 μm.

See also Figure S3.

progenitor cells (NPCs), and examined their reprogramming in the absence of Tets. As indicated in the AP colony-formation assay, neonatal keratinocytes [Tet1−/− Tet2−/− Tet3 f/−] could be reprogrammed efficiently upon conditional deletion of the only functional *Tet3* allele (Figures S3A–S3D). NPCs derived from TKO ESCs also underwent efficient programming (Figures S3E–S3H). Moreover, inactivation of floxed *Tet2*, in [Tet1−/− Tet2 f/f Tet3−/−] MEFs at a stage (days 4–6) subsequent to the MET did not seem to have any effect whereas earlier inactivation led to no AP-positive colonies (Figures S3I–S3K). These results demonstrate that the expression of the miR-200 family that is critical for the MET relies on Tet enzymes and that the inability of the Tet-deficient MEFs to be reprogrammed can be primarily attributed to a failure to activate their expression and initiate MET.

Impaired Oxidative Demethylation of miRNA Genes in Tet-Deficient MEFs

Having revealed the lack of miRNA reactivation as a major cause for blocking MET in Tet-deficient MEFs, we reasoned that persistent epigenetic silencing might have rendered these somatic cells unresponsive to reprogramming. The miR-200 family has two clusters in the mouse genome, with miR-200b, miR-200a, and miR-429 sharing one transcript and miR-200c

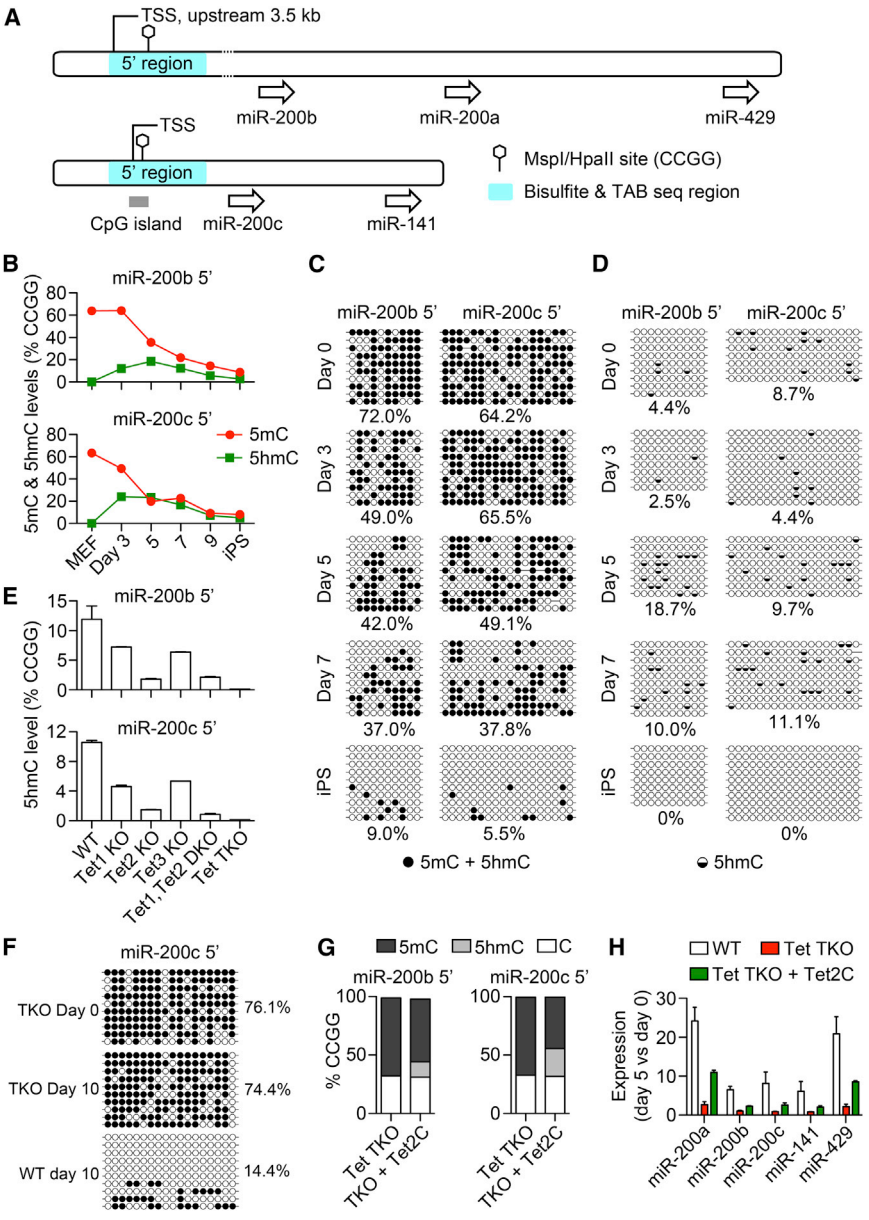

Figure 4. Tet-Dependent Oxidative Demethylation and Activation of MET-Related miRNA Genes

(A) Schematic illustration of the miR-200 family gene clusters. Hexagons denote the C(C)GG sites analyzed in the glucosylated hydroxymethyl-sensitive qPCR (GlucMS-qPCR) assay in (B), (E), and (G). TSS denotes putative transcription start sites.

(B) Dynamic regulation of methylation and hydroxylation at miR-200b and miR-200c 5′ region (putative promoter region) during reprogramming as reflected by the changes of the 5mC and 5hmC levels determined by GlucMS-qPCR assay. The y axis shows % of modification (5mC or 5hmC) in the C(C)GG site analyzed. The cells of days 3–9 were FACS-sorted SSEA1-positive cells.

(C) Profiles of 5mC + 5hmC in the putative promoter regions of miR-200b and miR-200c in cells before (MEF) and during reprogramming (OSK days 3, 5, and 7) revealed by bisulfite sequencing. The cells of days 3–7 were FACS-sorted SSEA1-positive cells.

(D) Profiles of 5hmC revealed by Tet-assisted bisulfite (TAB) sequencing. The cells of days 3–7 were FACS-sorted SSEA1-positive cells.

(E) Impaired 5mC hydroxylation in Tet-deficient MEFs. The y axis shows % of 5hmC in the C(C)GG site determined by GlucMS-qPCR assay. Data represent means ± SD of two independent experiments.

(F) Impaired demethylation in the 5′ region of miR-200c in TKO MEFs during reprogramming. MEFs or total cells under reprogramming at day 10 were analyzed by bisulfite sequencing.

(G) Restoration of 5mC hydroxylation in Tet-deficient MEFs by ectopic Tet2C. The 5hmC levels at the indicated miR loci in MEFs under reprogramming at day 5 were determined by GlucMS-qPCR assay.

(H) Partial rescue of miRNA activation in Tet-deficient MEFs under reprogramming by ectopic expression of the Tet2C. Data represent means ± SD of two independent experiments.

See also Figure S4.

and miR-141 sharing another (Figure 4A). In order to analyze the dynamics of DNA methylation during reprogramming, we sorted SSEA1-positive cells (1%–10% of the total population) at reprogramming days 3–9, which are considered a population poised to become iPSCs (Polo et al., 2012). In wild-type MEFs under reprogramming, the putative promoter loci (or 5′ region) of miR-200b and miR-200c and other examined loci within the gene body registered a dynamic reprogramming of DNA modifications as reflected in the results of the GlucMS-qPCR assay that quantifies 5mC and 5hmC at selected CCGG sites (Figure 4B; data not shown). The hypermethylation state decreases gradually, in parallel with the appearance of 5hmC, which peaked around day 5. Detailed bisulfite sequencing analysis in the 5′ regions of both clusters revealed hypermethylation in MEFs at the start (day 0), hypomethylation in iPSCs, and intermediate levels at days 3–7 (Figure 4C). Because conventional bisulfite sequencing cannot distinguish 5hmC from 5mC, we applied Tet-assisted bisulfite sequencing (Yu et al., 2012b) to analyze the occurrence of 5hmC. Strikingly, the 5hmC levels in day 5 MEFs undergoing reprogramming reached 18.7% and 9.7%, respectively, in the 5′ regions (Figure 4D). Most importantly, Tet triple knockout abolished 5hmC formation with Tet2 knockout (KO) having the greatest effect among the three individual knockouts (Figure 4E). As a consequence of failed hydroxylation, hypermethylation as exemplified by the 5′ region of miR-200c was still retained in TKO cells by day 10 (Figure 4F).

In order to gain a global view of the dynamics of methylcytosine and hydroxymethylcytosine during reprogramming, we performed reduced representation bisulfite sequencing (RRBS) and Tet-assisted-RRBS (TA-RRBS) of cellular DNA at reprogramming days 0 and 5. A marked increase in 5hmC was noticed in various genomic regions in the initial days, accompanying the

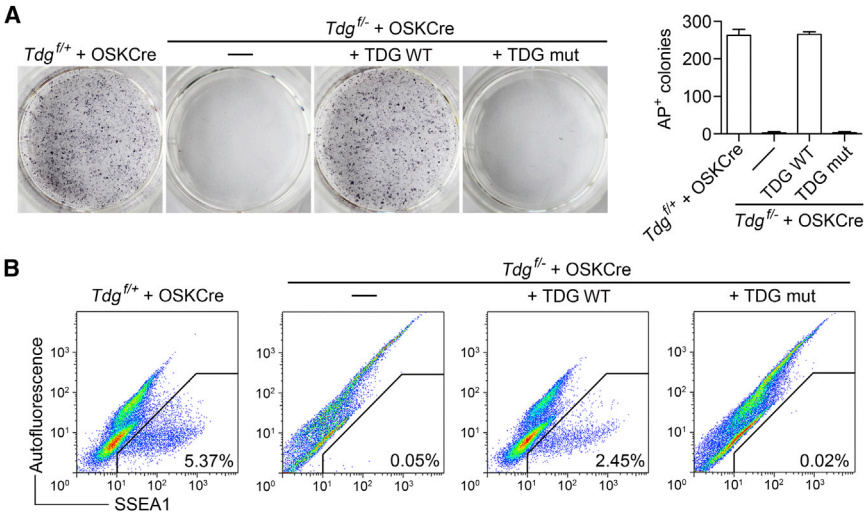

Figure 5. TDG Knockout Prevents Reprogramming of MEFs (see also Figure S5)

(A) AP staining of cells 10 days after transduction. Quantification of AP-positive colonies is shown at the right. MEFs with two *Tdg* genotypes (f/+ and f/−) were transduced with retroviral Oct4, Sox2, and Klf4 (OSK) reprogramming factors and the Cre-EGFP fusion. TDG-depleted MEFs (*Tdg* f/− + Cre) were also cotransduced with the wild-type (WT) or the mutant form (mut; N151A) of TDG to test for rescue. Data represent means ± SD of two independent experiments.

(B) Representative FACS plots of MEFs stained for SSEA1.

See also Figure S5.

decrease in 5mC (Figures S4A and S4B). An inverse correlation between 5hmC and 5mC was also seen among promoters (Figure S4C). Gene Ontology analysis indicated that the most-enriched promoters were associated with cell adhesion (Figure S4D), consistent with the idea that MET-related genes are a group of targets for Tet-catalyzed hydroxylation during the early phase of reprogramming. Among the enriched targets subject to methylation reprogramming were the miR-200 clusters (Figure S4E). Despite the fact that the *Oct4* locus also gained 5hmC (Figure S4E), the combined level of 5mC and 5hmC did not seem to decline and its expression was lacking in the early phase of reprogramming as shown in latter experiments.

A further functional validation of Tet enzymes in the epigenetic regulation of miRNAs was provided by the observation that ectopic expression of the Tet2 catalytic domain restored the 5hmC level in the 5′ regions of the two clusters in the TKO MEFs (Figure 4G) and resulted in upregulation of the miRNAs, albeit to a lesser degree than in the wild-type MEFs (Figure 4H). Taken together, these data demonstrate that Tet-dependent 5mC hydroxylation demethylates and reactivates MET-promoting miRNAs in reprogramming MEFs.

TDG Is Essential for MET and Reprogramming MEFs to iPSCs

DNA hydroxylation in reprogramming MEFs can have several ramifications for epigenetic regulation. Apart from the possibility of 5hmC serving as a stable mark, which is unlikely the major function of 5hmC predicated on its transitory occurrence, DNA demethylation may happen in part by hydroxylation, followed by passive dilution or further conversion to 5fC and5caC (He et al., 2011; Ito et al., 2011) and subsequent removal by an active mechanism. TDG is implicated in DNA demethylation initiated by Tet enzymes due to its ability to recognize and excise the higher oxidation products 5fC and 5caC (He et al., 2011; Maiti and Drohat, 2011), although the biological significance of the Tet-TDG functional connection has not been fully evaluated. We further extended our findings of the coupling between Tet and TDG by demonstrating their interdependency in the activation of a methylated reporter gene (Figure S5A). In order to explore the potential involvement of Tet-catalyzed higher oxidation in cell reprogramming, we established inducible *Tdg* knockout MEFs from embryos carrying a floxed and a null allele and tested them for iPSC induction. The Cre-mediated deletion of *Tdg* did not affect the proliferation of MEFs (Figure S5B). Upon transduction with Oct4, Sox2, Klf4, and Cre recombinase, the control MEFs with a wild-type *Tdg* allele in addition to a floxed allele showed a normal reprogramming capacity. However, MEFs carrying a null allele together with a floxed allele did not result in any iPSCs positive for AP and SSEA1 (Figures 5A and 5B). Re-expression of wild-type TDG, but not the catalytic mutant (N151A; Figure S5C), restored full reprogramming capacity (Figure 5).

Similar to the Tet TKO MEFs, TDG-null MEFs did not initiate the MET as judged by morphology and mesenchymal/epithelial marker expression (Figures 6A and 6B). Likewise, the blockage of MET initiation in *Tdg*-deficient MEFs could be ascribed to the failed activation of regulatory miRNAs (Figure 6C), and the MET resumed upon forced expression of miR-200c, but not Tet2C (Figure 6D). As evidenced by the formation of AP-positive colonies, robust reprogramming proceeded in the absence of TDG upon rescue with miR-200c or other two miRNAs, miR-200b and miR-429, with an efficiency of above 30% of the *Tdg*-proficient wild-type cells (Figure 6E). iPSC lines could be established from rescued *Tdg* KO MEFs (Figure 6F), and they were pluripotent as demonstrated by the generation of high-grade chimeric mice (Figure 6G). Contrary to the drastic effect on MEFs, *Tdg* deletion did not prevent keratinocyte and NPCs from reprogramming (Figures S6A–S6D). Cre-mediated late deletion from *Tdg*-floxed MEFs did not seem to impair the generation of AP-positive colonies whereas early deletion prior to MET led to no single colony (Figures S6E and S6F).

The data above led us to conclude that the TDG is required for MET by contributing to the reactivation of the critical miRNA genes in the early phase of reprogramming. Because the epigenetic regulation, MET, and iPSC formation in TDG-null MEFs all depend on the catalytic activity of TDG, we infer that the formation and excision of 5fC and 5caC are likely a critical step that at least partially contributes to the demethylation process.

Coordinated Action of Tet and TDG in Oxidative DNA Demethylation

In order to dissect the demethylation pathway underlying miRNA reactivation, we attempted to detect the higher oxidation

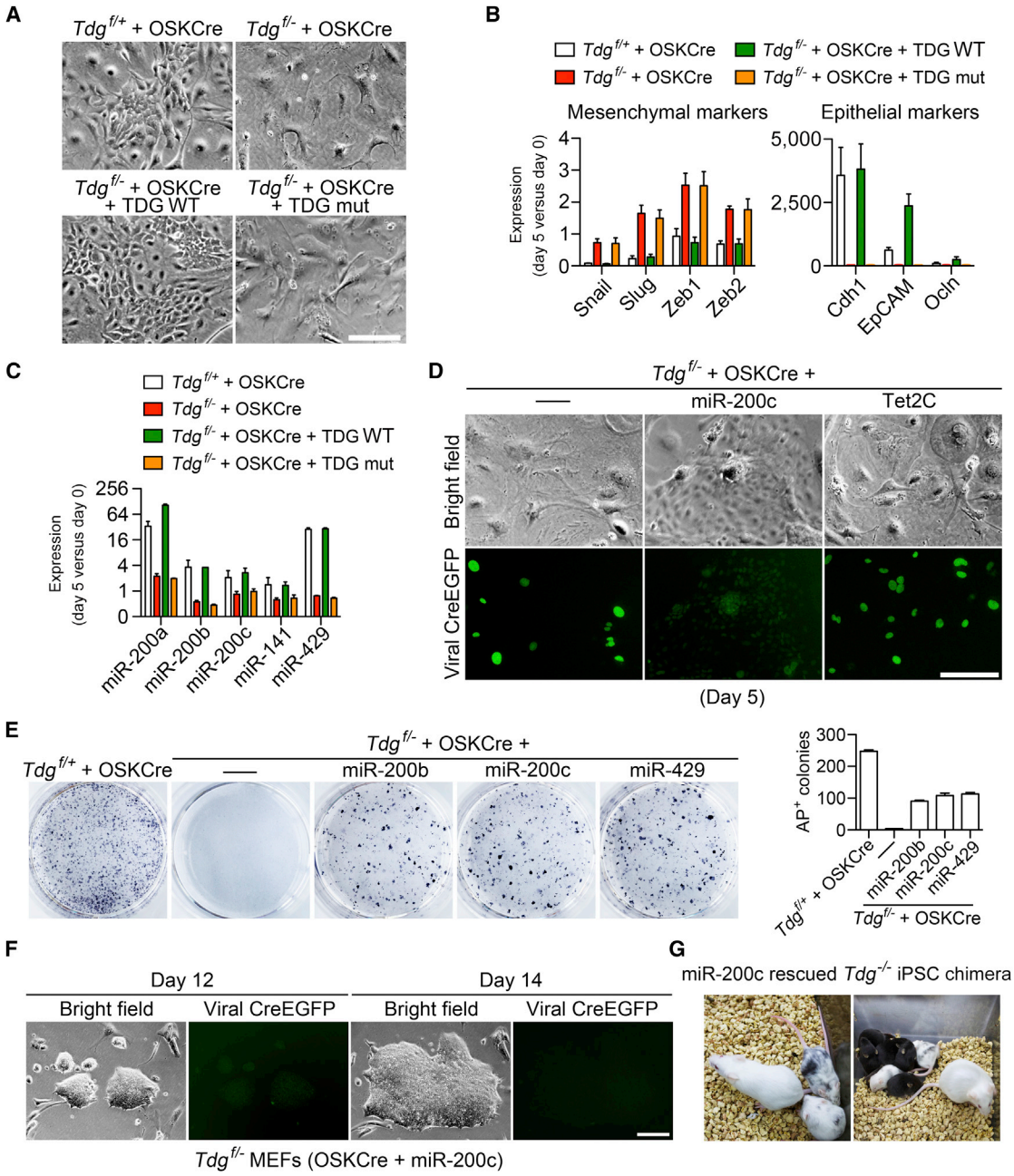

Figure 6. TDG Deficiency Blocks MET

(A) Lack of MET in MEFs depleted of TDG and rescue of MET upon re-expression of a functional TDG. Representative phase-contrast photographs of transduced MEFs (day 5) are shown. The scale bar represents 100 μm.

(B) Effect of TDG on the expression of mesenchymal and epithelial markers in MEFs under reprogramming at day 5. Expression levels were normalized to *Gapdh*. Data represent means ± SD of three independent experiments.

(C) Effect of TDG on the expression of the miR-200 family miRNAs in MEFs under reprogramming at day 5. The expression levels were normalized to *Rnu6*. Data represent means ± SD of three independent experiments.

(D) Restoration of MET in TDG-depleted MEFs upon ectopic expression of miR-200c. Note that the retroviral Cre-EGFP fusion gene is still weakly expressed at day 5 in intermediate MEFs rescued for MET by ectopic miR-200c expression. The scale bar represents 100 μm.

(E) AP staining of day 10 colonies arising from *Tdg f/+*, *Tdg f/−*, and *Tdg f/−* MEFs transduced with OSKCre with or without rescue by the indicated miRNA. AP-positive colony numbers are shown on the right. Data represent means ± SD of two independent experiments.

(F) Representative photographs of colonies induced from TDG-depleted MEFs rescued with the ectopic expression of miR-200c (days 12 and 14). Note the silencing of the retroviral CreEGFP fusion gene. The scale bar represents 100 μm.

(G) Photographs of chimeras generated from miR-200c-rescued *Tdg−/−* iPSCs. Rescued *Tdg−/−* iPSCs on a B6 genetic background were injected into ICR blastocysts.

See also Figure S6.

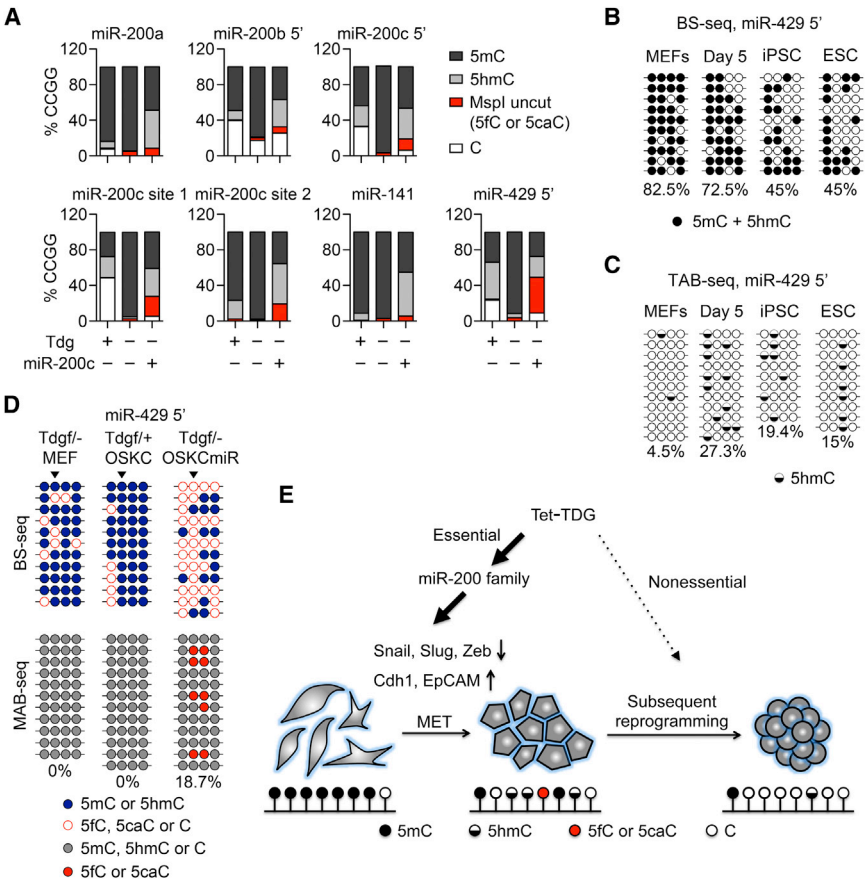

Figure 7. Dynamic Methylation Reprogramming through Coupled Action of Tet and TDG during Reprogramming

(A) GlucMS-qPCR analysis of cytosine modifications at the miR-200 family loci in intermediate cells from wild-type (+) and *Tdg*-deficient (–) MEFs rescued with (+) and without (–) ectopic miR-200c at reprogramming day 5. The level of combined 5fC and 5caC at a selected C(C)GG site was derived from the amount of DNA resistant to *Msp*I cleavage (*Msp*I uncut).

(B) Profiles of 5mC and 5hmC in the 5′ region of miR-429 during iPSC induction. Note that a significant proportion of the black circles ought to be 5hmC (compare to C), as 5hmC and 5mC are indistinguishable in this bisulfite-sequencing (BS-seq) analysis. Day 5 cells were unsorted population undergoing reprogramming.

(C) Profiles of 5hmC revealed by TAB-seq. Day 5 cells were unsorted population.

(D) MAB sequencing detection of 5fC and 5caC (red) in a 5′ region of miR-429 at reprogramming day 5 in indicated MEFs transduced with Cre (C) and with Cre-miR-200c (CmiR), respectively. BS-seq profiles are shown on the top for comparison. Untransduced *Tdg f*/– MEFs served as a control. In MAB-seq, 5fC and 5caC, which are resistant to M.*Sss*I methylation in vitro but sensitive to the subsequent bisulfite conversion, are read as "C" whereas all other forms (5mC, 5hmC, and C) are read as "5mC". Arrowheads indicate the selected C(C)GG site analyzed in (A).

(E) Proposed role of oxidative demethylation during somatic cell reprogramming. Tet- and TDG-mediated demethylation is required for the reactivation of miR-200 family genes known to be critical for MET at the initiation phase of reprogramming.

See also Figure S7.

derivatives of 5mC in reprogramming MEFs. We took advantage of the observation that 5fC/5caC modifications, but not 5mC and 5hmC, block *Msp*I (CCGG) restriction digestion (He et al., 2011; Ito et al., 2011) to estimate the frequency of 5fC/5caC at the specific *Msp*I sites located in the miR-200 loci (Figure 4A). Whereas TDG-proficient intermediate cells and unrescued TDG-deficient cells lacked detectable 5fC/5caC, these modified species were readily detected in TDG-deficient cells rescued for reprogramming with ectopic miR-200c (Figure 7A). The abundance of 5fC/5caC varied among different loci, with the highest level detected in the 5′ region of miR-429. Like those of miR-200b and miR-200c (Figures 4C and 4D), the 5′ region of miR-429 also exhibited hypermethylation in starting MEFs (Figure 7B) and methylation reduction while gaining 5hmC in reprogramming intermediates and iPSCs (Figure 7C).

In order to provide independent validation for 5fC/5caC deposition, we used a method for base-resolution profiling, termed methylation-assisted bisulfite sequencing (MAB-seq). The miR-429 region was selected due to the relative abundance of 5fC/5caC found at a CpG site in *Tdg*-null reprogramming cells (Figure 7A). MAB sequencing revealed a considerable amount (~19%) of 5fC and 5caC in TDG-null cells undergoing reprogramming upon miRNA rescue (Figure 7D). No 5fC/5caC was detected in corresponding TDG-proficient intermediate cells or control MEFs harboring an intact wild-type or a floxed *Tdg* allele. As the total level of 5fC, 5caC, and unmodified cytosines (C) in this region determined by conventional bisulfite profiling was 64.6%, C could be inferred to account for 45.9%. Compared to the high levels of combined 5mC and 5hmC in MEFs (around 80%; Figures 7B–7D), Tet-promoted 5mC oxidation in the rescued reprogramming *Tdg*-deficient cells had not only generated 5fC and 5caC accumulation but had also led to more unmodified cytosines, presumably by replication-dependent passive dilution of the resultant oxidation products.

In summary, the higher oxidation derivatives appeared dynamic in intermediate reprogramming stages primarily due to constant removal by TDG as well as passive dilution. They accumulated to a certain degree in TDG-knockout cells rescued for reprogramming by ectopic miR-200c. Tet-mediated oxidation of 5mC coupled with TDG-initiated base excision occurs in intermediate cells undergoing reprogramming, leading to the demethylation and reactivation of miRNA genes critical for MET (Figure 7E).

DISCUSSION

The physiological significance of DNA oxidation in epigenetic regulation has remained poorly understood, especially with regard to its importance in lineage commitment and cell reprogramming. Whereas previous reports have suggested the

involvement of Tet-mediated hydroxylation in somatic cell reprogramming (Costa et al., 2013; Doege et al., 2012; Gao et al., 2013), our work indicates that none of the individual Tet knockouts abolish the capacity of MEFs to be reprogrammed. The requirement for DNA oxidation can only be demonstrated by eliminating all three *Tet* genes simultaneously. Deletion of the glycosylase TDG also renders MEFs incapable of reprogramming due to an impediment to epigenetic activation of miRNAs crucial to mesenchymal-to-epithelial transition, as found in Tet-deficient MEFs.

DNA demethylation can proceed either by active removal or the passive dilution of methylcytosines and its derivatives, as a result of DNA replication. Recent studies document a prominent role of replication-coupled passive demethylation in cell-fusion-based reprogramming (Tsubouchi et al., 2013), early embryonic development (Inoue and Zhang, 2011), as well as primordial germ cell development (Hackett et al., 2012; Kagiwada et al., 2013; Seisenberger et al., 2012; Vincent et al., 2013). Contrary to these observations, we demonstrate that both Tet and TDG are essential for miRNA gene demethylation and factor-induced cell reprogramming, in support of an active mode of DNA demethylation. TDG, initially identified as a thymine DNA glycosylase, is not required for DNA repair but rather plays an important role in epigenetic regulation (Cortázar et al., 2011; Cortellino et al., 2011). A role in active demethylation has been proposed for TDG, based on its capability to specifically recognize and excise the Tet-generated higher oxidation products 5fC and5caC (He et al., 2011; Maiti and Drohat, 2011). While still lacking evidence in a physiological reprogramming setting, we suppose that Tet and TDG-mediated demethylation is likely to play a locus-specific role whereas replication-mediated passive demethylation is more prevalent in settings where genome-wide erasure has to occur efficiently.

In both experimental and natural reprogramming models, DNA demethylation has been intimately linked to the activation of pluripotency loci. In particular, cell fusion and iPSC induction experiments have implicated Tet-mediated hydroxylation in the epigenetic reactivation of silent pluripotency genes, a perceived bottleneck in the path toward the establishment of pluripotency (Doege et al., 2012; Piccolo et al., 2013). Oocyte Tet3 provides a reprogramming activity for pluripotency gene reactivation during the early embryonic development after nuclear transfer and natural fertilization (Gu et al., 2011). In this work, we also detect Tet-mediated 5hmC deposition at pluripotency loci in addition to other genes, including those related to cell adhesion, during iPSC induction of mouse fibroblasts (Figures S4 and S7). Interestingly, our genetic ablation studies indicate that Tet function is not essential for the demethylation and reactivation of pluripotency genes, as iPSCs can still be generated from Tet-deficient MEFs upon the rescue of MET by a single miRNA. Rather, Tet enzymes have an indispensable role in promoting demethylation and reactivation of miRNAs critical for the fibroblasts to be converted into epithelia at the onset of reprogramming, thus breaking down an epigenetic barrier imposed on the regulatory miRNA genes (Figure 7E). As Tet- or TDG-deficient cells expressing ectopic miRNAs are amenable to reprogramming, the activation of pluripotency genes presumably encompasses passive demethylation involving DNA replication. It is likely that both active (Tet-mediated) and passive (replication-dependent) demethylation mechanisms contribute to pluripotency gene demethylation for the reprogramming of wild-type cells.

Deletion of individual *Tet* genes, or *Tet1* and *Tet2* in combination, in mouse is compatible with embryonic development (Dawlaty et al., 2011, 2013; Gu et al., 2011). In light of the functional redundancy of the *Tet* genes as revealed in this experimental reprogramming system, the assessment of the biological significance of DNA oxidation in development awaits the generation and examination of triple knockout animals. Interestingly, a report by Song et al. (2013) published during the revision of this manuscript implicates the downregulation of Tet activity in the epigenetic inactivation of miR-200, which supposedly contributes to EMT in the process of mammary tumorigenesis and metastasis. It remains to be addressed whether and to what extent Tet- and TDG-mediated DNA demethylation control MET-related miRNAs and other important developmental regulators in physiological and disease processes.

EXPERIMENTAL PROCEDURES

Animal Use and Care

Animal procedures were carried out according to the ethical guidelines of the Institute of Biochemistry and Cell Biology.

Derivation of Tet-Deficient MEFs

To prepare *Tet1,Tet2,Tet3* triple knockout (TKO) MEFs, Tet TKO ESCs were labeled with constitutively expressing lentiviral GFP and then injected into mouse blastocysts to obtain chimeric E12.5 embryos. MEFs were isolated, and the GFP-positive cells were sorted by fluorescence-activated cell sorting (FACS). More information is available in Supplemental Experimental Procedures.

Retroviral Production and iPSC Induction

Retroviral production and infection followed the previously published protocol (Takahashi and Yamanaka, 2006). For retroviral production, Plat-E cells were seeded at 7×10^6 cells per 100 mm dish 1 day before transfection. Nine micrograms of pMXs-based retroviral constructs were transfected into Plat-E cells using Lipofectamine 2000 reagents (Invitrogen) according to the manufacturer's recommendations. Eight to ten hours later, the medium was replaced. Another 48 hr later, virus-containing supernatants were collected and filtered through a 0.45 μm polyvinylidene fluoride filter (Millipore) and supplemented with 4 μg/ml polybrene (Sigma). MEFs (seeded at 5×10^4 cells per each well in a 6-well plate 1 day before infection) were incubated with virus-containing supernatants for 12 hr. After two rounds of infection, cells were replated onto mitomycin-C-treated MEF feeder layers and the medium was changed into optimized medium (Chen et al., 2011). GFP-positive or alkaline-phosphatase-positive colonies were scored. Alkaline phosphatase staining was performed with NBT/BCIP (Roche).

In the Tet TKO MEFs rescue experiments using Tet1C, Tet2C, or Tet3C, cells were cultured with optimized medium without vitamin C.

For the establishment of miR-200c-rescued *Tet* TKO and *Tdg* KO iPSC lines, *Tet* TKO and *Tdg f/−* MEFs were transduced with OSK/miR-200c and OSKCre/miR-200c retroviruses, respectively. Cells under induction were cultured in optimized medium. iPSC colonies were picked, transferred onto feeder layers, and cultured in ESC medium supplemented with 2i and leukemia inhibitory factor.

Bisulfite Sequencing and TAB-Seq

For bisulfite sequencing, 100 ng of genomic DNA were treated with the EZ DNA Methylation-Direct Kit (Zymo Research). For Tet-assisted bisulfite sequencing (TAB-seq), genomic DNA was treated according to the protocol published recently (Yu et al., 2012a). Briefly, 1 μg of genomic DNA was sonicated into fragments of 300 bp to 1 kb in size. The fragments were then glucosylated, oxidized with recombinant mouse Tet1C, and treated with bisulfite sequentially. Specific genomic regions were PCR amplified and cloned into pMD-19T (Takara) for sequencing.

GlucMS-qPCR

Genomic DNA was extracted with the DNeasy Blood and Tissue kit (QIAGEN). Glucosylated hydroxymethyl-sensitive quantitative PCR (GlucMS-qPCR) was performed using the EpiMark 5-hmC and 5-mC Analysis Kit (New England Biolabs).

MAB-Seq

One microgram of genomic DNA was methylated by M.*Sss*I (NEB) following the NEB's instruction. Complete methylation of the DNA was confirmed by restriction analysis. The methylated DNA was then purified by phenol-chloroform extraction and bisulfite sequencing performed as described above. The methodology will be described elsewhere.

Flow Cytometry

Single-cell suspensions were obtained by repetitive pipetting and filtered through a 40 μm cell strainer. Cells were incubated with anti-mouse SSEA-1 PE (eBioscience) and analyzed on a FACS Aria (BD Biosciences). Data were analyzed with FlowJo software (Tree Star).

RNA Extraction, Reverse Transcription, and qPCR

Total RNA was extracted from cells with Trizol reagent (Life Technologies) and reverse-transcribed using the PrimeScript RT Reagent Kit with a gDNA Eraser according to manufacturer's instructions (Takara). Quantitative real-time PCR was performed using SYBR Premix EX Taq (Takara) on Bio-Rad CFX96. For the quantification of miRNA expression, total RNA was reverse-transcribed with the PrimeScript miRNA qPCR Starter Kit (Takara), and qPCR was performed following the vendor's instructions.

ACCESSION NUMBERS

The Gene Expression Omnibus accession number for the RRBS and TA-RRBS data reported in this paper is GSE52741.

SUPPLEMENTAL INFORMATION

Supplemental Information for this article includes Supplemental Experimental Procedures and seven figures and can be found with this article online at http://dx.doi.org/10.1016/j.stem.2014.01.001.

ACKNOWLEDGMENTS

We thank Jiemin Wong, Pentao Liu, and Colum Walsh for critical reading of the manuscript. This work was supported by grants from the Ministry of Sciences and Technology of China (2012CB966903 and 2014CB964802), the National Science Foundation of China (31230039 and 31221001), the "Strategic Priority Research Program" of the Chinese Academy of Sciences (XDA01010301), and the National Science and Technology Major Project "Key New Drug Creation and Manufacturing Program" of China (grant number 2014ZX09507-002) to G.-L.X.

Received: April 22, 2013
Revised: November 25, 2013
Accepted: December 26, 2013
Published: February 13, 2014

REFERENCES

Bagci, H., and Fisher, A.G. (2013). DNA demethylation in pluripotency and reprogramming: the role of tet proteins and cell division. Cell Stem Cell *13*, 265–269.

Chen, J., Liu, J., Chen, Y., Yang, J., Chen, J., Liu, H., Zhao, X., Mo, K., Song, H., Guo, L., et al. (2011). Rational optimization of reprogramming culture conditions for the generation of induced pluripotent stem cells with ultra-high efficiency and fast kinetics. Cell Res. *21*, 884–894.

Chen, J., Guo, L., Zhang, L., Wu, H., Yang, J., Liu, H., Wang, X., Hu, X., Gu, T., Zhou, Z., et al. (2013). Vitamin C modulates TET1 function during somatic cell reprogramming. Nat. Genet. *45*, 1504–1509.

Cortázar, D., Kunz, C., Selfridge, J., Lettieri, T., Saito, Y., MacDougall, E., Wirz, A., Schuermann, D., Jacobs, A.L., Siegrist, F., et al. (2011). Embryonic lethal phenotype reveals a function of TDG in maintaining epigenetic stability. Nature *470*, 419–423.

Cortellino, S., Xu, J., Sannai, M., Moore, R., Caretti, E., Cigliano, A., Le Coz, M., Devarajan, K., Wessels, A., Soprano, D., et al. (2011). Thymine DNA glycosylase is essential for active DNA demethylation by linked deamination-base excision repair. Cell *146*, 67–79.

Costa, Y., Ding, J., Theunissen, T.W., Faiola, F., Hore, T.A., Shliaha, P.V., Fidalgo, M., Saunders, A., Lawrence, M., Dietmann, S., et al. (2013). NANOG-dependent function of TET1 and TET2 in establishment of pluripotency. Nature *495*, 370–374.

Dawlaty, M.M., Ganz, K., Powell, B.E., Hu, Y.C., Markoulaki, S., Cheng, A.W., Gao, Q., Kim, J., Choi, S.W., Page, D.C., and Jaenisch, R. (2011). Tet1 is dispensable for maintaining pluripotency and its loss is compatible with embryonic and postnatal development. Cell Stem Cell *9*, 166–175.

Dawlaty, M.M., Breiling, A., Le, T., Raddatz, G., Barrasa, M.I., Cheng, A.W., Gao, Q., Powell, B.E., Li, Z., Xu, M., et al. (2013). Combined deficiency of Tet1 and Tet2 causes epigenetic abnormalities but is compatible with postnatal development. Dev. Cell *24*, 310–323.

Doege, C.A., Inoue, K., Yamashita, T., Rhee, D.B., Travis, S., Fujita, R., Guarnieri, P., Bhagat, G., Vanti, W.B., Shih, A., et al. (2012). Early-stage epigenetic modification during somatic cell reprogramming by Parp1 and Tet2. Nature *488*, 652–655.

Epsztejn-Litman, S., Feldman, N., Abu-Remaileh, M., Shufaro, Y., Gerson, A., Ueda, J., Deplus, R., Fuks, F., Shinkai, Y., Cedar, H., and Bergman, Y. (2008). De novo DNA methylation promoted by G9a prevents reprogramming of embryonically silenced genes. Nat. Struct. Mol. Biol. *15*, 1176–1183.

Gao, Y., Chen, J., Li, K., Wu, T., Huang, B., Liu, W., Kou, X., Zhang, Y., Huang, H., Jiang, Y., et al. (2013). Replacement of Oct4 by Tet1 during iPSC induction reveals an important role of DNA methylation and hydroxymethylation in reprogramming. Cell Stem Cell *12*, 453–469.

Goll, M.G., and Bestor, T.H. (2005). Eukaryotic cytosine methyltransferases. Annu. Rev. Biochem. *74*, 481–514.

Gregory, P.A., Bert, A.G., Paterson, E.L., Barry, S.C., Tsykin, A., Farshid, G., Vadas, M.A., Khew-Goodall, Y., and Goodall, G.J. (2008). The miR-200 family and miR-205 regulate epithelial to mesenchymal transition by targeting ZEB1 and SIP1. Nat. Cell Biol. *10*, 593–601.

Gu, T.P., Guo, F., Yang, H., Wu, H.P., Xu, G.F., Liu, W., Xie, Z.G., Shi, L., He, X., Jin, S.G., et al. (2011). The role of Tet3 DNA dioxygenase in epigenetic reprogramming by oocytes. Nature *477*, 606–610.

Gurdon, J.B., and Melton, D.A. (2008). Nuclear reprogramming in cells. Science *322*, 1811–1815.

Hackett, J.A., Sengupta, R., Zylicz, J.J., Murakami, K., Lee, C., Down, T.A., and Surani, M.A. (2012). Germline DNA demethylation dynamics and imprint erasure through 5-hydroxymethylcytosine. Science *339*, 448–452.

He, Y.F., Li, B.Z., Li, Z., Liu, P., Wang, Y., Tang, Q., Ding, J., Jia, Y., Chen, Z., Li, L., et al. (2011). Tet-mediated formation of 5-carboxylcytosine and its excision by TDG in mammalian DNA. Science *333*, 1303–1307.

Inoue, A., and Zhang, Y. (2011). Replication-dependent loss of 5-hydroxymethylcytosine in mouse preimplantation embryos. Science *334*, 194.

Ito, S., Shen, L., Dai, Q., Wu, S.C., Collins, L.B., Swenberg, J.A., He, C., and Zhang, Y. (2011). Tet proteins can convert 5-methylcytosine to 5-formylcytosine and 5-carboxylcytosine. Science *333*, 1300–1303.

Jaenisch, R., and Bird, A. (2003). Epigenetic regulation of gene expression: how the genome integrates intrinsic and environmental signals. Nat. Genet. Suppl. *33*, 245–254.

Kagiwada, S., Kurimoto, K., Hirota, T., Yamaji, M., and Saitou, M. (2013). Replication-coupled passive DNA demethylation for the erasure of genome imprints in mice. EMBO J. *32*, 340–353.

Li, J.Y., Pu, M.T., Hirasawa, R., Li, B.Z., Huang, Y.N., Zeng, R., Jing, N.H., Chen, T., Li, E., Sasaki, H., and Xu, G.L. (2007). Synergistic function of DNA methyltransferases Dnmt3a and Dnmt3b in the methylation of Oct4 and Nanog. Mol. Cell. Biol. *27*, 8748–8759.

Li, R., Liang, J., Ni, S., Zhou, T., Qing, X., Li, H., He, W., Chen, J., Li, F., Zhuang, Q., et al. (2010). A mesenchymal-to-epithelial transition initiates and is required for the nuclear reprogramming of mouse fibroblasts. Cell Stem Cell *7*, 51–63.

Maiti, A., and Drohat, A.C. (2011). Thymine DNA glycosylase can rapidly excise 5-formylcytosine and 5-carboxylcytosine: potential implications for active demethylation of CpG sites. J. Biol. Chem. *286*, 35334–35338.

Pastor, W.A., Aravind, L., and Rao, A. (2013). TETonic shift: biological roles of TET proteins in DNA demethylation and transcription. Nat. Rev. Mol. Cell Biol. *14*, 341–356.

Piccolo, F.M., Bagci, H., Brown, K.E., Landeira, D., Soza-Ried, J., Feytout, A., Mooijman, D., Hajkova, P., Leitch, H.G., Tada, T., et al. (2013). Different roles for Tet1 and Tet2 proteins in reprogramming-mediated erasure of imprints induced by EGC fusion. Mol. Cell *49*, 1023–1033.

Polo, J.M., Anderssen, E., Walsh, R.M., Schwarz, B.A., Nefzger, C.M., Lim, S.M., Borkent, M., Apostolou, E., Alaei, S., Cloutier, J., et al. (2012). A molecular roadmap of reprogramming somatic cells into iPS cells. Cell *151*, 1617–1632.

Samavarchi-Tehrani, P., Golipour, A., David, L., Sung, H.K., Beyer, T.A., Datti, A., Woltjen, K., Nagy, A., and Wrana, J.L. (2010). Functional genomics reveals a BMP-driven mesenchymal-to-epithelial transition in the initiation of somatic cell reprogramming. Cell Stem Cell *7*, 64–77.

Seisenberger, S., Andrews, S., Krueger, F., Arand, J., Walter, J., Santos, F., Popp, C., Thienpont, B., Dean, W., and Reik, W. (2012). The dynamics of genome-wide DNA methylation reprogramming in mouse primordial germ cells. Mol. Cell *48*, 849–862.

Seisenberger, S., Peat, J.R., Hore, T.A., Santos, F., Dean, W., and Reik, W. (2013). Reprogramming DNA methylation in the mammalian life cycle: building and breaking epigenetic barriers. Philos. Trans. R. Soc. Lond. B Biol. Sci. *368*, 20110330.

Song, S.J., Poliseno, L., Song, M.S., Ala, U., Webster, K., Ng, C., Beringer, G., Brikbak, N.J., Yuan, X., Cantley, L.C., et al. (2013). MicroRNA-antagonism regulates breast cancer stemness and metastasis via TET-family-dependent chromatin remodeling. Cell *154*, 311–324.

Tahiliani, M., Koh, K.P., Shen, Y., Pastor, W.A., Bandukwala, H., Brudno, Y., Agarwal, S., Iyer, L.M., Liu, D.R., Aravind, L., and Rao, A. (2009). Conversion of 5-methylcytosine to 5-hydroxymethylcytosine in mammalian DNA by MLL partner TET1. Science *324*, 930–935.

Takahashi, K., and Yamanaka, S. (2006). Induction of pluripotent stem cells from mouse embryonic and adult fibroblast cultures by defined factors. Cell *126*, 663–676.

Thiery, J.P., Acloque, H., Huang, R.Y., and Nieto, M.A. (2009). Epithelial-mesenchymal transitions in development and disease. Cell *139*, 871–890.

Tsubouchi, T., Soza-Ried, J., Brown, K., Piccolo, F.M., Cantone, I., Landeira, D., Bagci, H., Hochegger, H., Merkenschlager, M., and Fisher, A.G. (2013). DNA synthesis is required for reprogramming mediated by stem cell fusion. Cell *152*, 873–883.

Vincent, J.J., Huang, Y., Chen, P.Y., Feng, S., Calvopiña, J.H., Nee, K., Lee, S.A., Le, T., Yoon, A.J., Faull, K., et al. (2013). Stage-specific roles for tet1 and tet2 in DNA demethylation in primordial germ cells. Cell Stem Cell *12*, 470–478.

Wang, Y., Chen, J., Hu, J.L., Wei, X.X., Qin, D., Gao, J., Zhang, L., Jiang, J., Li, J.S., Liu, J., et al. (2011). Reprogramming of mouse and human somatic cells by high-performance engineered factors. EMBO Rep. *12*, 373–378.

Wang, G., Guo, X., Hong, W., Liu, Q., Wei, T., Lu, C., Gao, L., Ye, D., Zhou, Y., Chen, J., et al. (2013). Critical regulation of miR-200/ZEB2 pathway in Oct4/Sox2-induced mesenchymal-to-epithelial transition and induced pluripotent stem cell generation. Proc. Natl. Acad. Sci. USA *110*, 2858–2863.

Yu, M., Hon, G.C., Szulwach, K.E., Song, C.X., Jin, P., Ren, B., and He, C. (2012a). Tet-assisted bisulfite sequencing of 5-hydroxymethylcytosine. Nat. Protoc. *7*, 2159–2170.

Yu, M., Hon, G.C., Szulwach, K.E., Song, C.X., Zhang, L., Kim, A., Li, X., Dai, Q., Shen, Y., Park, B., et al. (2012b). Base-resolution analysis of 5-hydroxymethylcytosine in the mammalian genome. Cell *149*, 1368–1380.